Received: 5 February 2024 | Revised: 24 April 2024 | Accepted: 21 May 2024

DOI: 10.1002/cjce.25357

RESEARCH ARTICLE

THE CANADIAN JOURNAL OF CHEMICAL ENGINEERING

An investigation on hydrate prediction and inhibition: An industrial case study

Nejat Rahmanian[1] | **Nejmi Söyler**[2,3] | **Farai Munashe Wande**[1] | **Hamed Hashemi**[4]

[1]School of Engineering, Faculty of Engineering and Digital Technologies, University of Bradford, Bradford, UK

[2]Department of Chemical Engineering, Ondokuz Mayıs University, Samsun, Turkey

[3]Graduate School of Natural and Applied Sciences, Materials Science and Engineering, Ege University, Bornova, Turkey

[4]Department of Chemical and Metallurgical Engineering, University of the Witwatersrand, Johannesburg, South Africa

Correspondence
Nejat Rahmanian, School of Engineering, Faculty of Engineering and Digital Technologies, University of Bradford, Bradford, UK.
Email: n.rahmanian@bradford.ac.uk

Abstract

This investigation reports the first study to predict natural gas hydrate formation using both Aspen HYSYS® and HydraFlash software for various gas compositions and thermodynamic inhibitors (monoethylene glycol [MEG] concentrations at 10, 20, 30, and 40 wt.% and methanol concentrations at 10 and 20 wt.%). The simulated predictions are compared with the results of the experimental data in the literature. It has been shown that HydraFlash software can accurately predict hydrate formation conditions for a given industrial case, without having to carry out costly experimental work. This work also evaluated the effect of inhibitors and it appears that inhibitor type and concentration are determined according to condition of gas composition. MEG is consequently selected as the most ideal hydrate inhibitor for the industrial case. This also was confirmed through COSMO-RS studies in which the sigma profile and sigma potential of the considered inhibitors were obtained and presented using density functional (DFT) calculations to verify the hydrogen bonding affinities of the inhibitors to water molecules. HydraFlash was utilized to predict the dissociation conditions of hydrates under the influence of a high concentration of MEG inhibition, reaching up to 40 wt.% at 313 K and a pressure of 311.1 bar. Finally, it is shown that both software packages are quite accurate and useful tools for the prediction of hydrate for simple systems. However, HydraFlash can simulate more complex systems, including different types of salts at higher pressures. Investigation results indicate insightful guidance for accurately predicting hydrate dissociation under simulated conditions.

KEYWORDS

Aspen HYSYS®, gas hydrates, HydraFlash, thermodynamic inhibitors

1 | INTRODUCTION

The term natural gas is customarily reserved for gaseous minerals found in subsurface rock reservoirs, but all terrestrial gases such as air, volcanic emissions, and so forth are also called natural gases.[1] The composition of pipeline natural gas extracted from the source varies depending on the source and the processing of the gas. Generally, natural gas contains mostly methane and smaller proportions of ethane and other hydrocarbons.[2]

Inorganic compounds such as nitrogen, hydrogen sulphide, and carbon dioxide are undesired components when combined with water[3,4] and these wide varieties of small molecules can stabilize the crystal lattice of water.[5] Indeed, they form solid crystalline compounds known as gas hydrates, under suitable pressure–temperature conditions, which cause problems during the production, processing, and distribution of natural gas. Figure 1 shows typical pressure and temperature conditions of hydrate formation (Kelland[6]) and it is evident that as pressure increases, hydrates can form at temperatures as high as 25–30°C.

The gas processing operation occurs at conditions with low temperatures and high pressures, which will be within the hydrate stability zone. Hydrate control has received a considerable amount of attention due to the flow assurance subject in the gas and oil industry due to its ubiquitous nature.[3,7] If it is not addressed properly in design and operation, the result could be catastrophic.[8] This, in turn, has led to the regulation of gas water content and to the improvement of hydrate plugs prevention methods.[9,10] Moreover, one of the main concerns in the oil and gas industry has been the increasing costs associated with the inhibition of gas hydrate formation due to the development of offshore gas reservoirs.[11] Therefore, it is essential to predict the onset of hydrate formation for the economic and successful process of natural gas production operations.[12] Accordingly, hydrate management traditionally includes pipeline insulation, active heating, water removal, low pressure operation, or thermodynamic inhibitors—mainly methanol and monoethylene glycol (MEG).[13] These inhibitors work by shifting the gas hydrate stability curve to higher pressures or lower temperatures through reduction.[14] Thermodynamic hydrate inhibitors are so far the most common chemical class employed in the prevention of hydrate formation.[6,15,16] MEG and methanol (MeOH) are the two most common types of thermodynamic hydrate inhibitors, which are commonly used to prevent hydrate formation in production and process operations.[17] Diethylene glycol (DEG) and triethylene glycol (TEG) are sometimes employed in hydrate prevention but are less effective.[18] Methanol significantly partitions the gas and liquid hydrocarbon phases in comparison to glycols such as MEG, which partitions almost exclusively into the bulk water phase. Therefore, glycols are often preferred over methanol when the gas–oil–ratio (GOR) is high and water-cut low.[19] A typical measure of inhibitor effectiveness is subcooling, which is the difference between the hydrate formation temperatures with and without inhibitor.[20] Table 1 shows computed subcooling values for different thermodynamic inhibitors within the water phase (Kelland[6]). In order to determine the temperature and pressure in which the hydrate is in equilibrium, it is impractical to carry out experiments for each and every composition of gaseous mixtures,[21] and thus, various correlations have been presented in the literature to predict hydrate formation conditions.[22] Recently, there has been an increase in the use of artificial neural networks to study this problem,[23] mainly because of the reliability and high sensitivities of computer packages for the prediction of hydrate formation temperature and hydrate inhibition.

A number of researchers have predicted the conditions for hydrate formation in different ways such as: (a) the prediction of hydrate formation conditions for gas mixture systems using thermodynamics and artificial neural network modelling was presented by Rebai et al.[24]; (b) the gas hydrate efficiency of thermodynamic inhibitors was compared by Deka et al.[25] and a knowledgebase was obtained for cost-effective applications; (c) a gas consumption rate by calculating the driving force from the fugacity coefficient of the components in the gas phase was researched by Talaghat[21]; (d) the accuracy of the

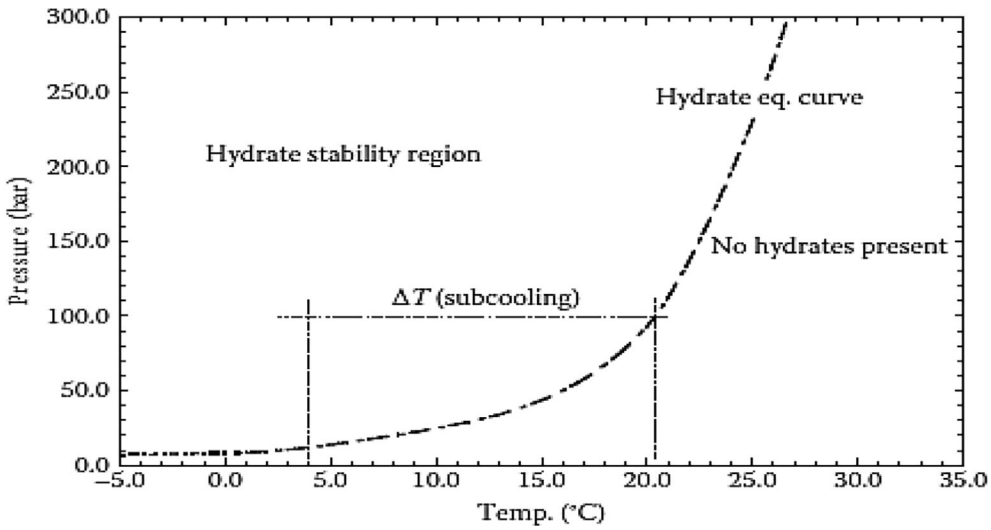

FIGURE 1 Typical natural gas hydrate formation pressure–temperature curve.[6]

TABLE 1 Subcooling values at the performance of various thermodynamic inhibitors in the water phase (Kelland[6]).

Chemical name	Methanol	Ethanol	Mono ethylene glycol	Diethylene glycol	Triethylene glycol	Sodium chloride	Potassium formate
Chemical formula	CH_3OH	C_2H_6O	$C_2H_6O_2$	$C_4H_{10}O_3$	$C_6H_{14}O_4$	NaCl	$CHKO_2$
CAS number	67-56-1	64-17-5	107-21-1	111-46-6	112-27-6	7647-14-5	590-29-4
Concentration (wt.%)	Depression of hydrate point (°C)						
5	2.0	1.4	1.05	0.63	0.46	1.96	–
10	4.2	3.0	2.25	1.4	1.05	4.3	2.5
20	9.3	6.6	5.2	3.3	2.7	10.7	7.1
30	15.3	10.7	9.0	5.9	5	15.0	12.9
35	18.6	13.0	11.35	7.5	6.5	–	–
40	22.2	15.4	14.0	9.3	8.2	–	–

new methane–pure water system correlation was enhanced by Riazi et al.[26] on the basis of experimental data gathered by Sloan and Koh[27] and they used the Matlab curve fitting software to optimize the solution; (e) hydrate formation temperature was predicted in natural gas binary mixtures using the group method of the data handling approach and all models were performed by Behvandi et al.[28]; and (f) the distribution of pressure and pressure gradient under different operating conditions were explored by Yang et al.[29] and the accuracy of the simulation model was evaluated with lab experiment data. Given the wide range of differing simulation approaches taken by the various applied methods, different simulation packages have their own characteristics and advantages. Thereby, prediction tools should be selected appropriately according to the proper conditions and system in the initial stage. The challenges existing in the current research structure are discussed and the potential future research directions are proposed. To the best of our knowledge, this is the first study to compare HydraFlash and Aspen HYSYS® for the prediction of hydrate formation. This is the first evaluation of a real industrial case with such a large throughput. The case study was chosen from the plan that the first author was working on where he observed a major challenge during design stage to evaluate hydrate prediction and inhibition.

The aim of the current study is to simulate an industrial case condition in the South Pars Gas Project (Iran) using HydraFlash and Aspen HYSYS® and to investigate the phase behaviour of hydrocarbon fluids in an oil and gas pipeline with various inhibitors. The main objective of this study is to compare the predictions from HydraFlash and Aspen HYSYS®. HydraFlash was developed at Heriot-Watt University, which was later improved and commercialized by Hydrafact,[30] UK, while Aspen HYSYS®[31] is a commercial package provided by the Aspenone group. Four different gas compositions during the summer and winter seasons were simulated, and the results of the phase equilibrium data from the simulation were validated against plant data. The effect of thermodynamic inhibitors on natural gas hydrate formation was investigated to determine the best minimal inhibitor concentration. Finally, experimental methane hydrate equilibrium data for mixed sodium chloride and ethylene glycol aqueous solution were used to evaluate the simulation packages in more challenging systems. In the evaluation of hydrate dissociation conditions, it is imperative to consider the potential implications of utilizing inhibitors at elevated concentrations. The selection of inhibitor concentrations as high as 40 wt.% in our study was motivated by the need to comprehensively assess the predictive capabilities of the models under extreme conditions. While such concentrations may appear unusually high compared to typical usage levels, they were chosen to explore the models' performance across a wide range of inhibitor concentrations and to provide insights into their effectiveness under challenging scenarios. It is important to note that in industrial applications, there may be instances where high inhibitor concentrations are required to achieve significant temperature shifts and prevent hydrate formation. Our study aims to shed light on the predictive capabilities of the models under these conditions and highlight potential implications associated with higher inhibitor concentrations. Ultimately, the insights gained from our study can inform decision-making processes and aid in the development of effective strategies for hydrate mitigation and process optimization.

2 | METHODOLOGY

2.1 | Selection of experimental data from the literature

In this work, the HydraFlash and Aspen HYSYS® software are used and the simulation outputs were compared with the results of an experimental data by Deaton and Frost[32] for the simple hydrocarbon system. They built a high-pressure glass-windowed rig to facilitate the study of natural gas hydrates with different gas compositions. The glass window enabled them to observe the formation of hydrates and their phase equilibrium in natural gas pipelines. Experimental data typically allows the researcher to interpret their effects on the variables. We used the compositional data for the industrial case in the South Pars Project. The operating condition composition of feed at the inlet of the subsea pipeline at the offshore platform is provided in Table 2. We also extend the work to a more complex system in the South Pars Project, Iran, which includes salts. Industrial data evolves more defined insights and experiences. The hydrate dissociation measurements by Masoudi et al.[33] were used for a real and complex system of aqueous solution of NaCl-EG, as presented in Table 3. The presence of salts causes it to be challenging to study the thermodynamic properties under industrial conditions. Experimental results were generated by step-heating, where the system temperature was raised in steps and only equilibrium (stable pressure) data were used to determine dissociation conditions.

2.2 | COSMO-RS study

The primary mechanism of the gas hydrate inhibitors is to distract water molecules by forming hydrogen bonds with them. COSMO-RS is a strong tool capable of predicting the tendency of a compound for creating hydrogen bonding, and hence it can be used as a screening tool to examine the inhibition effect of different inhibitors prior to any experimental measurement. COSMO-RS is regarded as the best link between chemical engineering thermodynamics and chemical quantum mechanics. The idea was developed in the early 1990s by Klamt and Schüürmann assuming a surface charge around the molecule or ion, which can be obtained using so-called COSMO calculations.[34] These surface charges can be converted to the interaction parameters between species, which can be used in the calculation of fluid properties. In order to produce the COSMO surface charges for the studied inhibitors required in the calculation of interaction parameters (Klamt[35]), the inhibitors' structures need to be optimized first. For the purpose of this study, the Amsterdam density functional (ADF) framework (Baerends[36]) has been used in which, the Beck-Perdew (BP) GGA level of density functional theory along with triple zeta polarized (TZP) basis set, the Klamt radii, and the Delly surface area for atoms were used in the calculations. After the geometry optimization step, the COSMO files were generated using the final optimized structure.[35,37]

2.3 | Simulation procedure

Commercial process simulators are normally used in the predicting the conditions for hydrate formation and they compute the chemical activity of the water phase, the effect of higher molecular hydrocarbons, and the effect of hydrate inhibitors. Further, process simulations rely on existing packages and thermodynamic equations to estimate hydrate formation at various conditions. For oil, gas, and petrochemical applications, the Peng–Robinson equation of state (EoS) is generally used for the calculation of fugacity in the vapour and liquid phases. In this study, the Peng–Robinson equation of state[38] was used for estimating water fugacity in the vapour and liquid phases. The following equation was obtained for the estimation of the fugacity of water in the fluid phases, f_i[38–41]:

$$\ln\frac{f_i}{z_iP}=\frac{b_i}{b_m}(Z-1)-\ln(Z-B)-\frac{\alpha}{2\sqrt{2}}\left(\frac{1}{n}\frac{\partial n^2a}{\partial n_i}-\frac{b_i}{b_m}\right)\ln\left(\frac{Z+2.414B}{Z-0.414B}\right) \quad (1)$$

where

$$\frac{1}{n}\frac{\partial(n^2a)}{\partial ni}=\alpha b_i\mathrm{RT}+\frac{\partial(n\alpha)}{\partial(n_i)}b_m\mathrm{RT} \quad (2)$$

$$\frac{\partial(n\alpha)}{\partial n_i}=\frac{1}{(q_1+\alpha q_2)}\left(q_1\alpha_i+\ln\gamma_i+q_2\left(\alpha_i{}^2+\alpha^2\right)+\ln\frac{b_m}{b_i}+\frac{b_i}{b_m}-1\right) \quad (3)$$

$$B=\frac{b_mP}{\mathrm{RT}} \quad (4)$$

$$z_i=\frac{n_i}{\sum n_j}=\frac{n_i}{n} \quad (5)$$

$$\frac{\partial(nb_m)}{\partial n_i}=b_i \quad (6)$$

in which n stands for the number of moleculesn z_i stands for the mole fraction of component i, and Z presents the compressibility factor. For the evaluation of the activity

TABLE 2 Industrial natural gas composition and simulation model.

Property				Value
Normal flow, kmol/h				6.04E+04
Normal flow, Kg/h				1.30E+06
Pressure, bar				125
Temperature, °C				73.72
Molecular weight				21.54
Heat flow, kcal/h				−1.22E+09
Vapour				
Molar flow, kmol/h				5.86E+04
Normal flow, kg/h				1.17E+06
Density, kg/m^3 @ P, T				102
Liquid				
Standard liquid volume flow, m^3/h				203.9
Normal flow, kg/h				1.31E+05
Composition				
Components	**Formula**	**CAS number**	**Mole fraction**	**Model**
Methane	CH_4	74-82-8	0.83154	Peng–Robinson equation of state
Ethane	C_2H_6	74-84-0	0.05262	
Propane	C_3H_7	2025-55-0	0.01741	
i-Butane	C_4H_{10}	75-28-5	0.00380	
n-Butane	C_4H_{10}	106-97-8	0.00640	
i-Pentane	C_5H_{12}	78-78-4	0.00260	
Carbon dioxide	CO_2	75042-80-7	0.01781	
Nitrogen	N_2	7727-37-9	0.03001	
Hydrogen sulphide	H_2S	7683-06-4	0.00480	
Benzene	C_6H_6	71-43-2	0.00020	
Cyclohexane	C_6H_{12}	110-82-7	0.00040	
Methylcyclopentane	C_6H_{12}	5310-57-6	0.00030	
Methylcyclohexane	C_7H_{14}	108-87-2	0.00080	
Methylmercaptan	CH_4S	17719-48-1	0.00040	
Toluene	C_7H_8	108-88-3	0.00030	
p-Xylene	C_8H1_0	106-42-3	0.00140	
n-Pentane	C_5H_{12}	109-66-0	0.00260	
n-Hexane	C_6H_{14}	110-54-3	0.00300	
n-Heptane	C_7H_{16}	142-82-5	0.00320	
n-Octane	C_8H_{18}	111-65-9	0.00350	
n-Nonane	C_9H_{20}	111-84-2	0.00300	
n-Decane	$C_{10}H_{22}$	124-18-5	0.00240	
n-Undecane	$C_{11}H_{24}$	1120-21-4	0.00570	
Water	H_2O	7732-18-5	0.00580	

coefficient of the gas phase and water in Equation (3), γ_i, the electrolyte NRTL (eNRTL)[41] activity model was applied.

CSMHYD is also another package where the Van der Walls and Platteeuw method is postulated as a statistical model for hydrate formation. In this study the fugacity of

TABLE 3 Experimental methane hydrate dissociation conditions for sodium chloride-ethylene glycol.[33]

Sodium chloride concentration (mass%) CAS number 7647-14-5	Ethylene glycol concentration (mass%) CAS number 107–21-1	Dissociation point	
		Temperature (±0.1 K)	Pressure (±0.008 MPa)
15.0	21.3	262.3	5.068
		268.4	11.431
		274.3	27.758
		277.9	46.698

water in the hydrate phase (H) is calculated using the vdWP model as follows:

$$f_w^H = f_w^\beta \exp\left(\frac{-\Delta\mu_w^{\beta-H}}{RT}\right) \quad (7)$$

in which $\Delta\mu_w^{\beta-H}$ shows the difference between the chemical potential of the meta-stable β-phase and the actual hydrate phase, as explained in Section 2.3. The fugacity of the meta-stable β-phase, f_w^β, can be obtained using the following equation[42]:

$$f_w^\beta = f_w^{l\,o} \exp\left(\frac{-\Delta\mu_w^{\beta-l}}{RT}\right) \quad (8)$$

in which, $f_w^{l\,o}$ presents the fugacity of pure water in the liquid phase. The following equation is used to calculate the chemical potential difference between the empty hydrate lattice and the liquid phase, $\Delta\mu_w^{\beta-l}$, as indicated below:

$$\frac{\Delta\mu_w^{\beta-l}}{RT} = \frac{\Delta\mu_w^0}{RT} - \int_{T_0}^{T} \frac{\Delta h_w^{\beta-l}}{RT} dT + \int_{P_0}^{P} \frac{\Delta v_w^{\beta-l}}{RT} dP \quad (9)$$

where the reference temperature and pressure (T_0 and P_0) are set equal to 273.15 K and the vapour pressure of the ice, respectively. Since P_0 is small compared to the hydrate equilibrium pressure, it is usually set equal to zero. $\Delta\mu_w^0$ defines the difference in the chemical potential of water in the empty hydrate lattice and liquid phase at T_0. $\Delta h_w^{\beta-l}$ presents the molecular enthalpy difference between the meta-stable β-phase and liquid water or ice and $\Delta v_w^{\beta-l}$ is the molecular volume difference between the meta-stable β-phase and liquid water or ice. $\Delta h_w^{\beta-l}$ contains two parts, including the enthalpy of phase change from ice to liquid water at T_0 and a heat capacity contribution due to the heating of the liquid from T_0 to the corresponding temperature, T:

$$\Delta h_w^{\beta-l} = \Delta h_w^0 + \int_{T_0}^{T} \Delta C_{pw} dT \quad (10)$$

The foundation of the CSMHYD package was developed by Sloan.[43] Thus, as mentioned, the foundation of the current models that are currently employed is incorporated within Aspen HYSYS® (V8.0). In this study, Aspen HYSYS® (V8.0) was employed in combination with HydraFlash (version 3.3) in the prediction of hydrate formation under various conditions. Ayansola et al.[44] concluded that Aspen HYSYS® is an accurate hydrate prediction package, and this was further corroborated by Carroll[45] who states that it is an accurate tool that can predict hydrate formation to an error of 0.8°C. In this work, the Peng–Robinson EoS was used in both Aspen HYSYS® and HydraFlash for all the simulations that were carried out.

2.4 | Influence of process parameters

The data shown in Table 4 of various natural gas compositions are referenced as gases A, B, C, and D. Figure 2 shows their corresponding phase equilibrium obtained experimentally. The free water forms an ideal or nonideal mixture with the hydrate particles and can dissolve foreign substances.[46] Aspen HYSYS® allows for the assumption of free water for hydrate prediction, but HydraFlash does not have this facility and thus a mole fraction of 0.2 of water was assumed. Once the curves had been obtained, both HydraFlash and Aspen HYSYS® were employed in the prediction of the inhibition effect on gas B and simulations were carried out with MEG concentrations at 20 and 40 wt.%. As such, the obtained prediction for gas B shows the best appropriate precaution with 6.14% safety offset. Table 2 shows the tabulated compositional data for the industrial case in the South Pars Project. Aspen HYSYS® and HydraFlash were also employed in the prediction of hydrate formation conditions for this composition. HydraFlash was then employed in the prediction of formation conditions with inhibition. The hydrate formation predictions were carried out with MEG concentrations at 10, 20, 30, and 40 wt.% and nethanol at concentrations of 10 and 20 wt.%.

CH_4	C_2H_6	C_3H_8	C_4H_{10}	CO_2	H_2S	N_2	Component
0.654	0.127	0.103	0.037	0.002	0	0.077	Gas A
0.879	0.044	0.049	0.015	0.002	0	0.011	Gas B
0.91	0.032	0.02	0.031	0.004	0	0.003	Gas C
0.878	0.04	0.021	0.015	0.0325	0.0025	0.011	Gas D

TABLE 4 Concentration of different natural gases components (Deaton and Frost[32]).

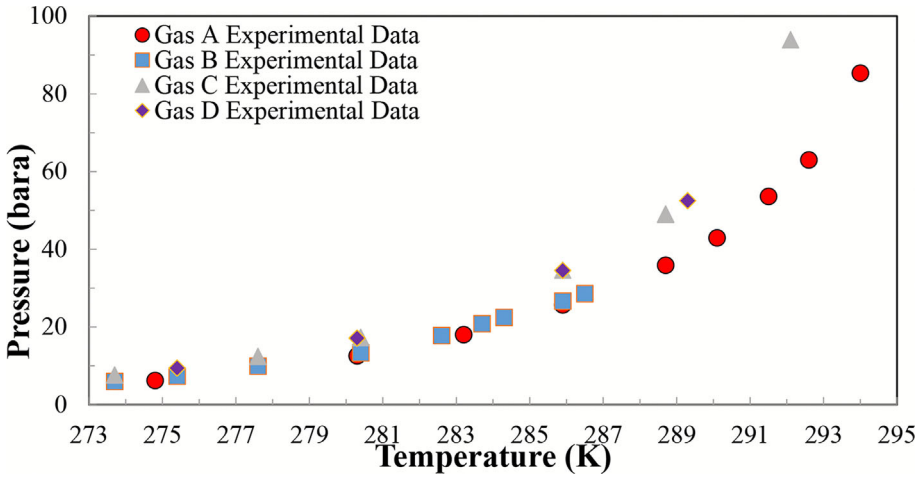

FIGURE 2 Experimental phase equilibrium data (Deaton and Frost[32]).

3 | RESULTS AND DISCUSSION

3.1 | Comparison of the hydrate prediction against experimental data

Figure 3A–D compare the experimental data for gases A, B, C, and D with the output of two software. Aspen HYSYS® can predict hydrate formation with an average error of 0.8°C since the solubility of the various components in the gas is neglected,[45] while Ayansola et al.[44] concluded that Aspen HYSYS® is an accurate hydrate prediction package. This is validated as the results show that the predicted hydrate formation values for Aspen HYSYS®, especially in Figure 3A, match the experimental data between 273 and 287 K where a deviation occurs. The remaining plots reveal that all of the prediction curves for both Aspen HYSYS® and HydraFlash fall to the left of the experimental data. Due to the importance of obtaining accurate predictions, both simulation packages could be simulated with a safety percentage offset. It is within the software that offers an appropriate precaution and adds a safety factor almost 10% towards the hydrate-forming region.[47] Figure 3B shows that simulated output values are less sensitive to temperature in the range 273–287 K. Figure 3C shows that simulated equilibrium curves fall to the left of experimental data between 285 and 292 K. Simulation results in Figure 3D show P–T line predicts temperatures for the gas D slightly over experimental data, especially between 281 and 289 K. The results represent that the hydrate formation prediction conditions from HydraFlash and Aspen HYSYS® are almost identical since the difference in hydrate predictions is less than a 10% confidence interval opposite to the experimental results. It shows that each software package provides accurate predictions of hydrate dissociation for gases A, B, C, and D with average error 0.19%, 6.14%, 1.9%, and 1.67%, respectively.

3.2 | Evaluation of the hydrate formation curves with inhibition for an experimental phase equilibrium data

Figure 4 shows hydrate formation predictions for gas B with MEG inhibition. The plots show that HydraFlash and Aspen HYSYS® yield the same hydrate formation curves. Due to this, it can be concluded that HydraFlash can accurately predict the formation of hydrates since Aspen HYSYS® predictions have been validated by Ayansola et al.[44] and Carroll.[43]

Table 2 shows the composition of natural gas for an industrial case in the South Pars Gas Project, Iran. Aspen HYSYS® and HydraFlash have the same hydrate formation curves as shown in Figure 5 for this case. Aspen HYSYS® could not predict the hydrate formation past 296.30 K while HydraFlash can predict beyond this temperature.

Figure 6 compares the hydrate formation curves for gas B with MEG (20 and 40%wt) and methanol (20 and 40%wt) inhibition. The predicted hydrate formation

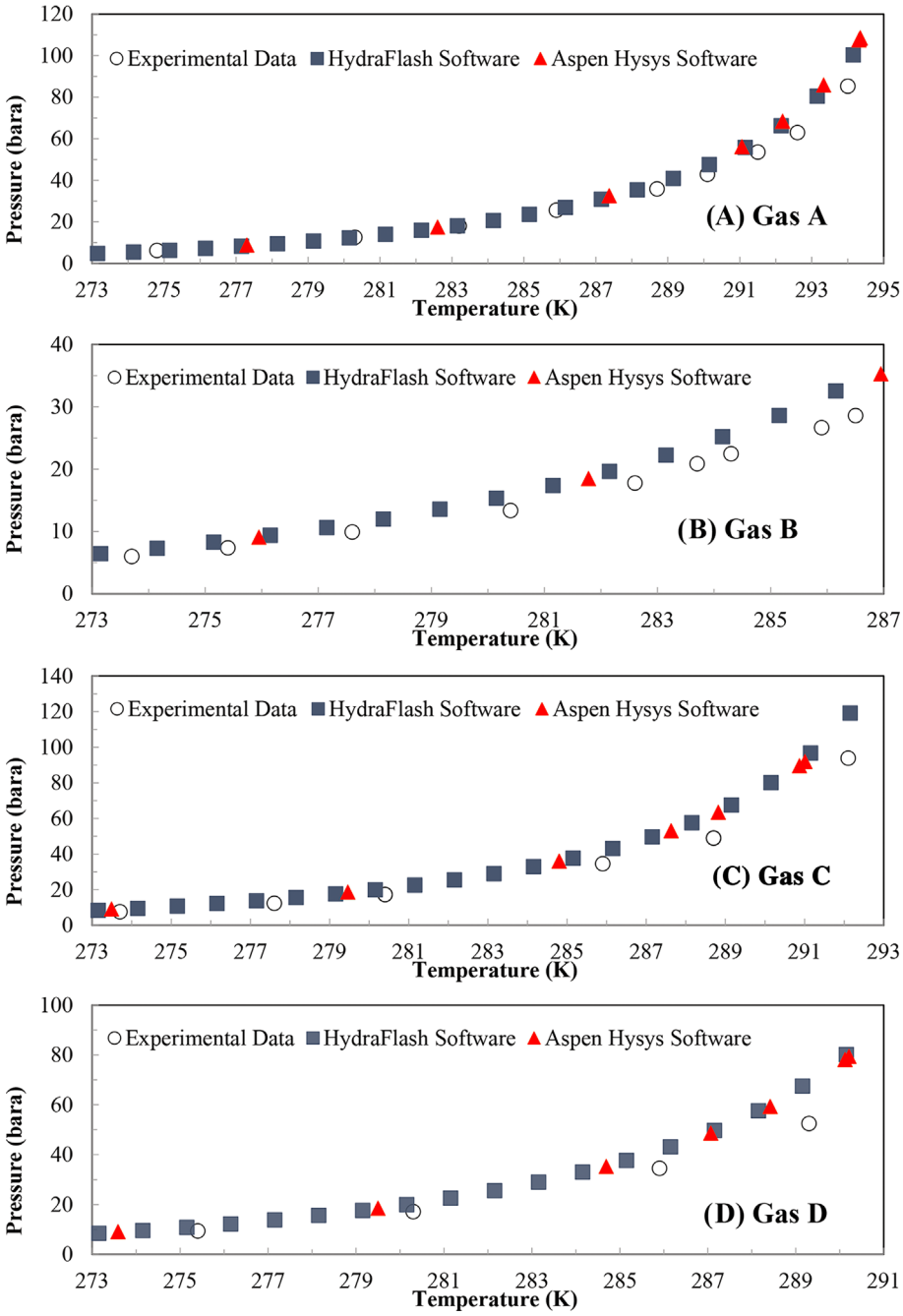

FIGURE 3 (A–D) Experimental data of the different natural gases components with Hysys and HydraFlash softwares.

curves are as expected as mentioned by Kelland[6] and as shown in Table 1, methanol provides greater subcooling than MEG.

3.3 | Effect of thermodynamic inhibition in various concentrations for an industrial case

Figure 7A,B show that the HydraFlash hydrate formation curves for the industrial case composition with 10 wt.% MEG and 10 wt.% methanol inhibition, respectively. The results in Figure 6 show that sub-cooling due to MEG is higher than that with methanol. Methanol has a high vapour pressure, so when the water cut is low, a large amount of methanol goes to the gas phase, and because of reducing its concentration in the aqueous phase, the inhibition effect occurs. Kelland[6] stated that glycols are preferred over methanol where the GOR (gas–oil–ratio) is high and water-cut low since MEG partitions appreciably into the bulk water phase while methanol does not. The amount of gas dissolved in the oil is high for the industrial case composition at operation conditions and has a low water cut due to the MEG partitioning coefficient,

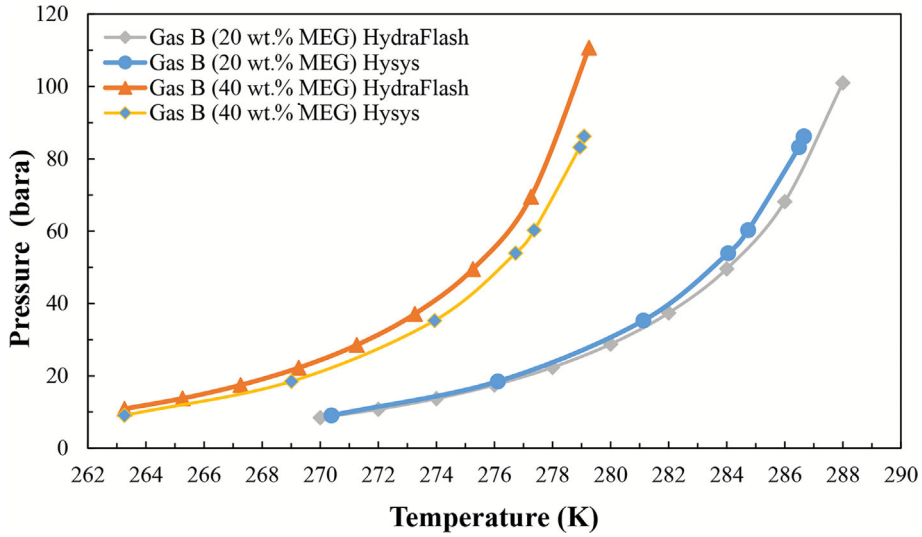

FIGURE 4 HydraFlash and HYSYS hydrate formation prediction with MEG inhibition for gas B.

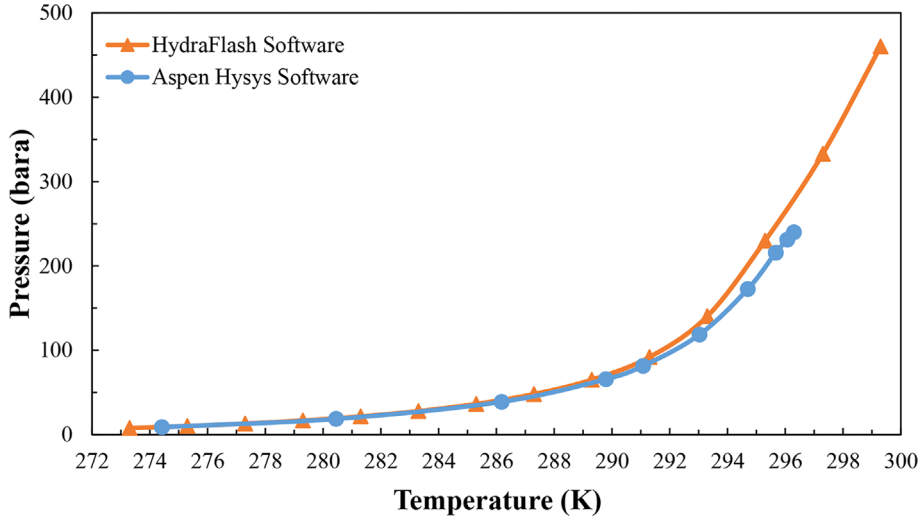

FIGURE 5 HYSYS and HydraFlash hydrate formation prediction for the industrial case.

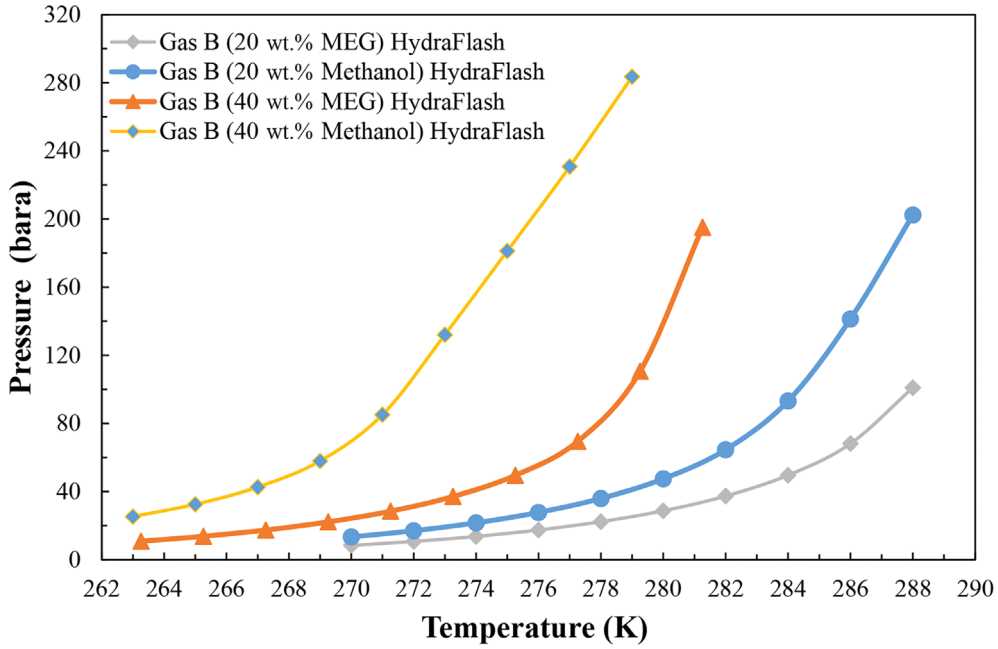

FIGURE 6 HydraFlash hydrate formation prediction with monoethylene glycol (MEG) and methanol inhibition for gas B.

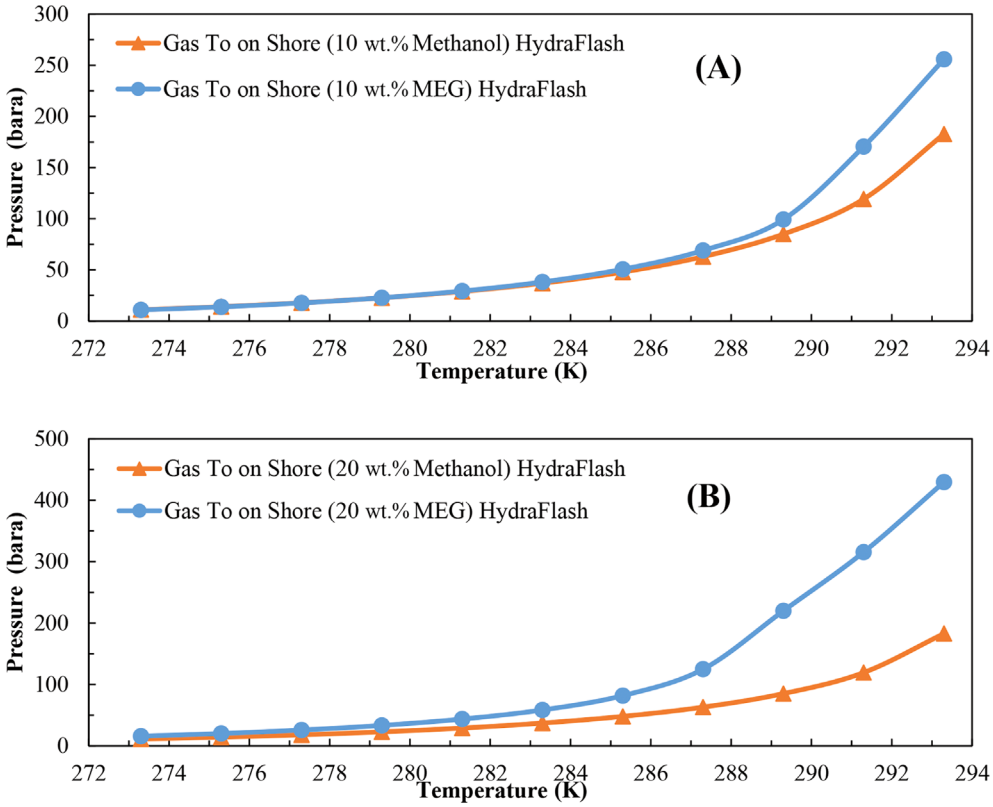

FIGURE 7 (A, B) HydraFlash hydrate formation prediction with 10 and 20 wt.% monoethylene glycol (MEG) and methanol inhibition for the industrial case.

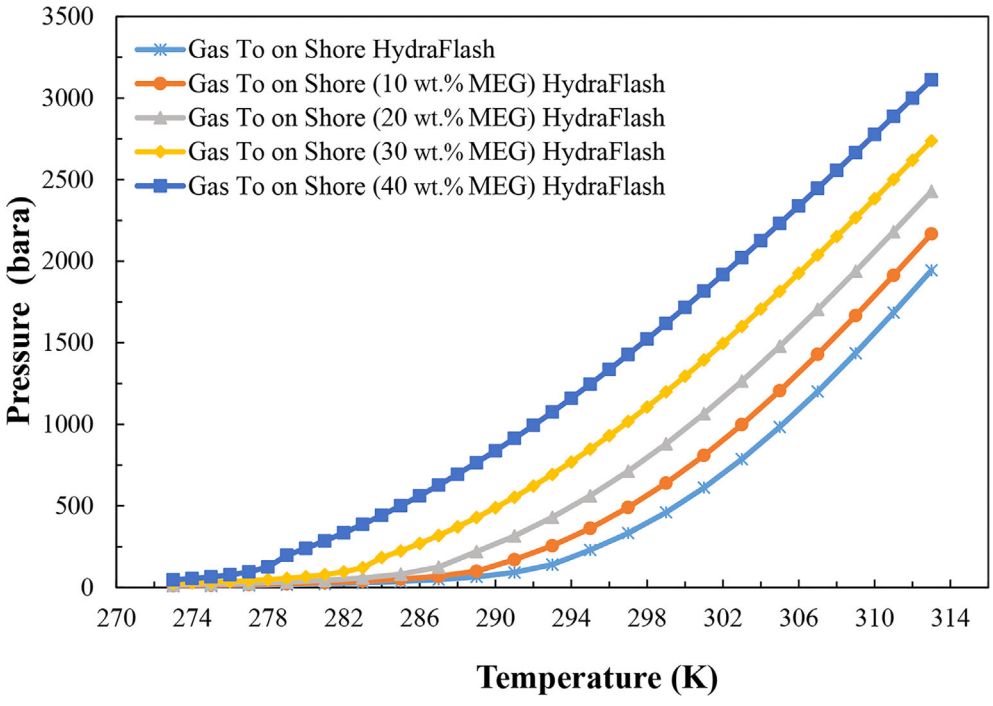

FIGURE 8 HydraFlash hydrate formation prediction with monoethylene glycol (MEG) for the industrial case.

which is exclusively higher subcooling than methanol to distribute the bulk water phase, as shown in Figure 7A,B. Gas B does not have a low water-cut, and as a result, methanol has higher sub-cooling in comparison to MEG, as shown in Figure 6. Based on the hydrate formation curves given in Figure 7A,B, MEG is selected as the most suitable hydrate inhibitor.

There are also other reasons that MEG is used as a hydrate inhibitor, most importantly because MEG can be regenerated. Alharooni et al.[48] stated that thermal

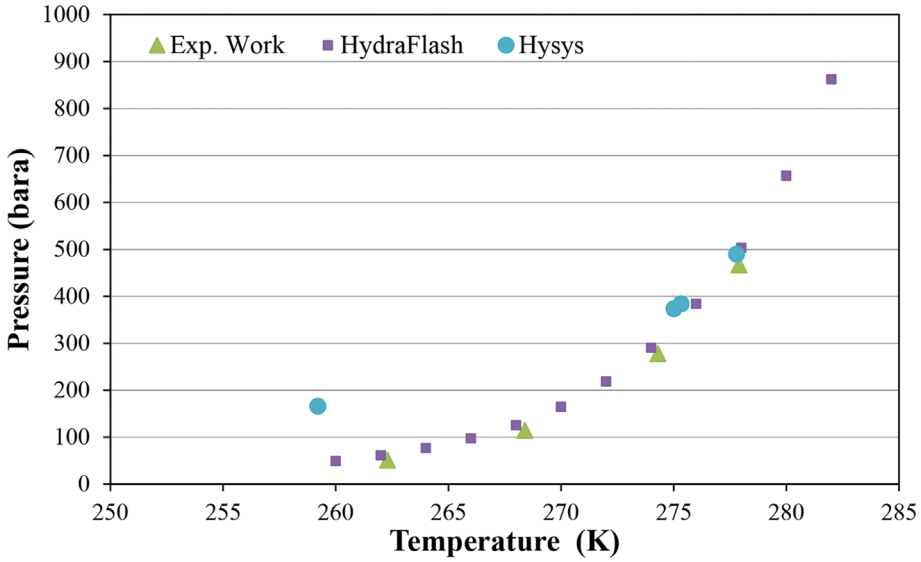

FIGURE 9 HydraFlash and HYSYS hydrate formation prediction for NaCl-EG aqueous solution.

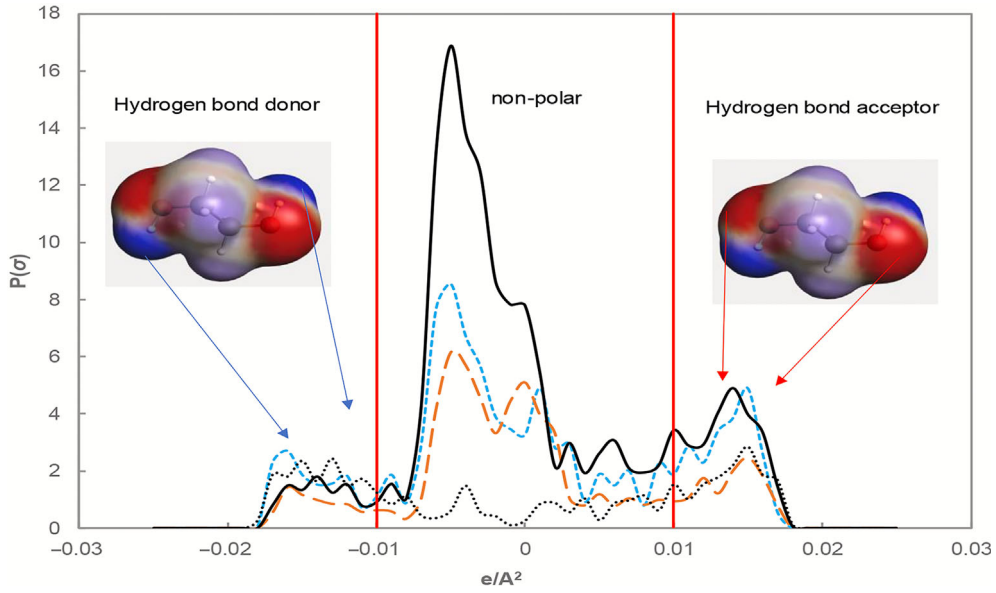

FIGURE 10 σ-Surface and σ-profiles of some commercially used inhibitors.

degradation of MEG may occur during the regenerating process when heated to high temperatures at the boiler. Figure 8 shows the hydrate formation curves with MEG as the inhibitor for various concentrations and up to 313 K with a pressure of 3111 bar for 40 wt.% MEG inhibition. Aspen HYSYS® could not predict formation curves with inhibition as a computational error always occurred due to the free water phase in the mole fraction.

3.4 | Predicting hydrate dissociation conditions in the presence of aqueous solution of NaCl-EG

In this section, Aspen HYSYS® (V8.0) was employed in combination with HydraFlash and predictions are validated against experimental data for the hydrate inhibition effect of aqueous solutions containing NaCl and ethylene glycol. Figure 9 shows experimental and predicted hydrate formation conditions for an aqueous solution of ethylene glycol. HydraFlash predictions show a good match with experimental data while Aspen HYSYS® match the experimental data from 275 to 278 K, but there are significant deviations at 259 K. It should be emphasized that Aspen HYSYS® predictions have not been used in the behaviour of aqueous solutions containing both salts and ethylene glycol. So far Aspen Hysys software included only salt as sodium chloride in the package and other types of salts such as calcium chloride, sodium sulphate, and magnesium chloride are not supported in the package. The advantage of HydraFlash is that it covers a wide range of salts

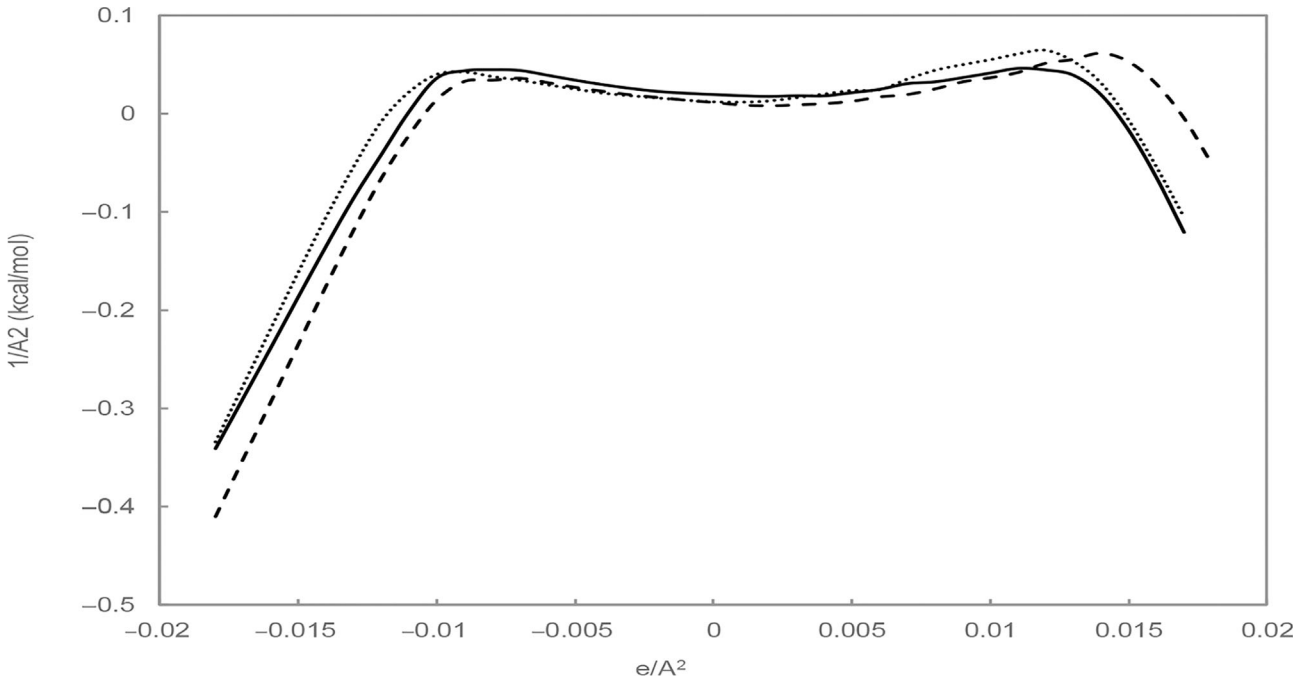

FIGURE 11 σ-Potentials of some commercially used inhibitors.

(13 types) and is specifically designed for hydrate prediction, though the software could be improved with respect to interface and documentation.

3.5 | COSMO-RS sigma (σ) profile and sigma (σ) potential

COSMO-RS σ-profile, σ-potential, and σ-surface are decent indicators in the pre-screening of the hydrogen bonding energies for gas hydrate mitigation. The σ-surface, σ-profile, and σ-potential deliver an excellent description of ion interaction behaviour with water by visualizing their electro-negativity and electro-positivity. The sigma surface of MEG and the sigma profiles of MEG, DEG, and methanol are depicted in Figure 10 for gas hydrate studies. The blue area on the σ-surface of MEG describes a strong negative (hydrogen bond [HB] donors), which corresponds to the area ≥ -0.1 eV·Å^{-2} in Figure 10. The red area shows a strong positive (≤ 0.1 eV·Å^{-2}) of HB-acceptors and the purple area designates the nonpolar nature of the compound ($-0.1 <$ non-polar ≤ 0.1 eV·Å^{-2}).[35] Water and commercially used inhibitors (MeOH, DEG, MEG) show two peaks of hydrogen affinity (donor and acceptor) resulting in a strong hydrogen bonding with water molecules. The hydrogen bonding strength that results in a better inhibition effect follows the trend MEG > DEG > MeOH. Figure 11 represents the σ-potential of the studied inhibitors. σ-potential delivers similar but more distinctive hydrogen bonding affinities compared to σ-profile. The same trend for the hydrogen bonding strength as that of the sigma profile can be observed in the sigma potential graph.

4 | CONCLUSIONS

In this paper, hydrate formation predictions made by HydraFlash and Aspen HYSYS® software have been presented and compared with the experimental data. There is a good agreement between the predictions and experimental results especially for simple hydrocarbon systems. The simulation packages were also employed to predict hydrate formation conditions in the prediction of inhibition effect on gas B. Predicted hydrate formation curves are as expected and methanol has provided a subcooling that is higher than MEG. However, the same simulation was carried out with an industrial case and the results show that MEG subcooling has a greater effect than methanol inhibition. HydraFlash predictions for especially a high concentration of MEG inhibition at 40 wt.% also showed that MEG is selected as the most ideal hydrate inhibitor for the industrial case. As a result, the typical measure of various thermodynamic inhibitors' effectiveness within the water phase is the difference and thermodynamic inhibitors' function in the prevention of hydrate formation is a key importance due to the distribution of the inhibitor between the gas and liquid phases.

For a complex system including various types of salts, HydraFlash software is more practical as it supports 12 different types of salts than the Aspen HYSYS. Further study of the inhibition effect of the inhibitors is carried out using the COSMO-RS model in which the hydrogen bonding strength of the inhibitors is examined using sigma profile and sigma potentials. It was found that MEG shows a better hydrogen bonding affinity resulting in a more inhibition effect compared to methanol and DEG.

AUTHOR CONTRIBUTIONS

Nejat Rahmanian: Supervision; writing – review and editing. **Nejmi Söyler:** Investigation; writing – review and editing; software. **Farai Munashe Wande:** Software; investigation. **Hamed Hashemi:** Software; investigation.

ACKNOWLEDGEMENTS

The authors would also like to thank the Turkish National Agency for offering an Erasmus student grant for Mr. Nejmi Söyler under the Erasmus+ Program Action 1 throughout the training period.

PEER REVIEW

The peer review history for this article is available at https://www.webofscience.com/api/gateway/wos/peer-review/10.1002/cjce.25357.

DATA AVAILABILITY STATEMENT

The data that support the findings of this study are available from the corresponding author upon reasonable request.

ORCID

Nejmi Söyler https://orcid.org/0000-0002-4279-4262

REFERENCES

[1] J. Carroll, *Natural Gas Hydrates: A Guide for Engineers*, Elsevier Science, Oxford **2009**.
[2] A. Demirbas, *Methane Gas Hydrate*, Springer-Verlag Limited, London **2010**.
[3] A. Farhadian, A. Shadloo, X. Zhao, R. S. Pavelyev, K. Peyvandi, Z. Qiu, M. A. Varfolomeev, *Fuel* **2023**, *336*, 1.
[4] B. Guo, A. Ghalambor, *Natural Gas Engineering Handbook*, Elsevier Science, Oxford **2012**.
[5] I. B. A. Sfaxi, V. Belandria, A. H. Mohammadi, R. Lugo, *Chem. Eng. Sci.* **2012**, *84*, 602.
[6] M. A. Kelland, *Production Chemicals for the Oil and Gas Industry*, 2nd ed., CRC Press, Boca Raton, FL **2014**.
[7] Z. Liu, B. Sun, Z. Wang, J. Zhang, X. Wang, *Fuel* **2021**, *291*, 120116.
[8] K. Kinnari, J. Hundseid, X. Li, K. M. Askvik, *J. Chem. Eng. Data* **2014**, *60*, 437.
[9] J. Wang, Y. Meng, B. Han, Z. Liu, L. Zhang, H. Yao, Z. Wu, J. Chu, L. Yang, J. Zhao, Y. Song, *Chem. Eng. J.* **2023**, *461*, 142020.
[10] G. Zahedi, Z. Karami, H. Yaghoobi, *Energy Convers. Manage.* **2009**, *50*, 2052.
[11] S. Shahnazar, N. Hasan, *Fluid Phase Equilib.* **2014**, *379*, 72.
[12] M. Atilhan, S. Aparicio, F. Benyahia, E. Deniz, *Advances in Natural Gas Technology*, Intech, Croatia **2012**.
[13] N. Daraboina, S. Pachitsas, N. Solms, *Fuel* **2015**, *148*, 186.
[14] H. Delavar, A. Haghtalab, *Fluid Phase Equilib.* **2013**, *338*, 100.
[15] C. W. Foo, L. Ruan, X. Lou, *J. Nat. Gas Sci. Eng.* **2016**, *35*, 1587.
[16] A. M. Teixeira, L. d. O. Arinelli, J. L. de Medeiros, O. d. Q. F. Araújo, *J. Nat. Gas Sci. Eng.* **2018**, *52*, 166.
[17] D. Sloan, *Natural Gas Hydrates in Flow Assurance*, Gulf Professional Publishing, Houston, TX **2011**.
[18] A. Khalifa, A. Barifcani, D. Pack, R. Gubner, V. Ghodkay, *J. Pet. Sci. Eng.* **2015**, *135*, 608.
[19] G. Lei, L. Li, H. A. Nasr-El-Din, presented at SPE Improved Oil Recovery Symposium. **2011**.
[20] C. Giavarini, K. Hester, *Gas Hydrates: Immense Energy Potential and Environmental Challenges*, Springer Science & Business, Berlin **2011**.
[21] M. R. Talaghat, *J. Nat. Gas Sci. Eng.* **2014**, *52*, 18.
[22] M. M. Ghiasi, A. Bahadori, S. Zendehboudi, A. Jamili, *J. Nat. Gas Sci. Eng.* **2013**, *15*, 69.
[23] M. Ghavipour, M. Chitsazan, S. H. Najibi, *Chem. Eng. Res. Des.* **2013**, *91*, 264.
[24] N. Rebai, A. Hadjadj, A. Benmounah, A. S. Berrouk, S. M. Boualleg, *J. Pet. Sci. Eng.* **2019**, *182*, 106270.
[25] B. Deka, A. Barifcani, A. Al Helal, D. Badi, V. Mahto, H. Vuthaluru, *J. Pet. Sci. Eng.* **2021**, *199*, 108312.
[26] S. H. Riazi, H. Heydari, E. Ahmadpour, A. Gholami, *J. Nat. Gas Sci. Eng.* **2014**, *18*, 377.
[27] E. D. Sloan, C. A. Koh, *Clathrate Hydrates of Natural Gases*, CRC Press, Boca Raton, FL **2008**.
[28] R. Behvandi, A. Tatar, A. Shokrollahi, A. Zeinijahromi, *Geoenergy Sci. Eng.* **2023**, *224*, 211634.
[29] L. Yang, H. Fu, H. Liang, Y. L. Wang, G. Han, K. Ling, *J. Pet. Sci. Eng.* **2019**, *183*, 106173.
[30] Hydrafact, *Phase Behaviour and PVT Properties of Petroleum Resorvoir Fluids*, Heriot-Watt University, Edinburgh **2013**.
[31] Hyprotech, *Tutorials and Application*, HYSYS, Edinburgh **2002**.
[32] W. M. Deaton, E. M. Frost, *Gas Hydrates and Their Relation to the Operation of Natural-Gas Pipe Lines. Bureau of Mines*, Helium Research Center, Amarillo, TX (USA) **1946**.
[33] R. Masoudi, B. Tohidi, R. Anderson, R. Burgass, J. Yang, *Fluid Phase Equilib.* **2004**, *219*, 157.
[34] A. Klamt, G. Schüürmann, *J. Chem. Soc., Perkin Trans.* **1993**, *1*, 799.
[35] A. Klamt, *J. Chem. Eng. Data* **2005**, *51*, 1480.
[36] E. J. Baerends, *J. Chem. Phys.* **2018**, *149*(5), 1.
[37] K. Z. Sumon, A. Henni, *Fluid Phase Equilib.* **2011**, *310*, 39.
[38] R. Stryjek, J. Vera, *Can. J. Chem. Eng.* **1986**, *64*, 323.
[39] P. Proust, J. Vera, *Can. J. Chem. Eng.* **1989**, *67*, 170.
[40] H. Hashemi, S. Babaee, A. H. Mohammadi, P. Naidoo, D. Ramjugernath, *J. Chem. Thermodyn.* **2015**, *80*, 30.
[41] C. C. Chen, Y. Song, *AIChE J.* **2004**, *50*, 1928.

[42] J. H. v. d. Waals, J. C. Platteeuw, *Advances in Chemical Physics*, John Wiley & Sons, Inc., Hoboken, NJ **2007**, p. 1.
[43] J. Carroll, *Natural Gas Hydrates-A Guide for Engineers*, Elsevier Science, Burlington **2003**.
[44] Y. E. Ayansola, D. O. Araromi, A. O. Arinkoola, K. K. Salam, *International Journal of Engineering Sciences* **2013**, *2*, 327.
[45] J. Carroll, *Gas Liquids Engineering* **2004**, *3*, 1.
[46] A. K. Sengupta, *Ion Exchange and Solvent Extraction*, CRC Press, Boca Raton **2011**.
[47] I. Ismail, V. Gaganis, D. Marinakis, R. Mousavi, B. Tohidi, *Chemical Thermodynamics and Thermal Analysis* **2023**, *9*, 100103.
[48] K. Alharooni, A. Barifcani, D. Pack, R. Gubner, V. Ghodkay, *J. Pet. Sci. Eng.* **2015**, *135*, 608.

How to cite this article: N. Rahmanian, N. Söyler, F. M. Wande, H. Hashemi, *Can. J. Chem. Eng.* **2025**, *103*(1), 396. https://doi.org/10.1002/cjce.25357